EARTH'S CRYOSPHERE
SCIENTIFIC JOURNAL

Kriosfera Zemli, 2019, vol. XXIII, No. 4, pp. 37–44 **http://www.izdatgeo.ru**

PROPERTIES OF FROZEN GROUND AND ICE

DOI: 10.21782/EC2541-9994-2019-4(37-44)

SHELF SEDIMENTS OF THE KARA SEA: COMPOSITIONS AND MICROSTRUCTURE

O.S. Kalashnikova[1], A.N. Kurchatova[1,2], E.A. Slagoda[1,2]

[1] *Earth Cryosphere Institute, Tyumen Scientific Centre, SB RAS, 86, Malygina str., Tyumen, 625000, Russia; olga.gasheva.91@mail.ru*
[2] *Tyumen Industrial University, 38, Volodarskogo str., Tyumen, 625000, Russia*

The shelf sediments of the Kara Sea sampled along two profiles, northward from the Spindler Cape (Yugor Peninsula) and W–E between Spindler and the Marresale Cape (western Yamal Peninsula) have been investigated by several methods: laser particle-size analysis, powder X-ray diffractometry, and electron microscopy. The bottom sediments belong to the marine, coastal, and continental facies distinguished on the basis of lithology, mineralogy, morphology, and signatures of cryogenic weathering. The signatures of cryogenesis revealed in the sediments are attributed to coast retreat or ice rafting.

Arctic shelf, Kara Sea, bottom sediments, microstructure, cryogenesis

INTRODUCTION

The Arctic shelf is a zone of Russia's strategic interest. This is the longest marine national frontier where a number of military objects are constructed for security reasons, while the shelf stores about 70 % of oil and gas resources, the key export item of the country. Investigation of Arctic shelf sediments has both theoretical and practical applications: data from the area make reference for construction on permafrost, which requires the knowledge of soil properties, and can provide clues to environments and history of regional Late Quaternary deposition. The relevant theoretical aspects have been subjects of numerous publications and international research, but they have focused mostly on glacial deposits from islands and landmass. The obtained data were commonly extrapolated to the shelf, without due regard for the specificity of marine deposition and available offshore field data.

Engineering-geological studies of the Russian Arctic shelf began in the 1980s for the purposes of petroleum exploration within the Barents-Kara province. The presence of permafrost on the shelf was first proven by drilling near the northwestern shore of the Yamal Peninsula and in the Pechora Sea [*Gritsenko and Bondarev, 1994*]. Studies of the offshore and coastal Arctic territories have furnished a wealth of data on the structure, composition, and mechanic properties of shelf sediments [*Soloviev, 1988; Neizvestnov and Reshetova, 1990; Danilov, 1992; Melnikov and Spesivtsev, 1995; Neizvestnov et al., 2012*].

The history of shelf permafrost and the role of transgressions in its degradation are among key debatable issues in the Arctic paleogeography [*Shpolyanskaya et al., 2006; Rokos, 2008*]. According to many existing models, the shelf permafrost formed in subaerial conditions during large-scale Late Valdai (Sartan) regression. However, there is evidence for recent origin of ice-rich sediments, i.e., data from the southeastern Barents and southwestern Kara Seas [*Maslov, 1988; Melnikov et al., 1998*], as well as from the Laptev Sea [*Kassens et al., 2000*].

We report new data on the composition and microstructure of bottom sediments sampled by gravity coring in the Kara shelf during a trip of the I.S. Gramberg Russian Research Institute of Marine Geology and Mineral Resources (*VNIIOkeangeologiya*, St. Petersburg) on R/V *Ivan Petrov* in the summer of 2007 [*Vanstein et al., 2008*].

MATERIALS AND METHODS

The samples were collected along two profiles in the Kara shelf (Fig. 1): an N–S profile northward from the Spindler locality, Yugor Peninsula (K-I), and a W–E profile from the Spindler locality through the Baidaratskaya Guba Bay to the Marresale Cape in the western shore of the Yamal peninsula (K-II).

Sampling for particle sizes and mineralogy of sediments was performed by gravity coring at each geological survey station. Temperatures were measured at every 10 cm all along the core section; samples were selected from the upper, middle, and lower section parts. The sea depths offshore from the Spindler locality vary from 22 to 220 m. The water temperatures changed during the survey season from 8.6 °C near the surface to –1.76 °C near the bottom, and the ground temperature in the shallow-sea part of the profile was –1.2 °C. The sea depths along the other profile, opposite the Marresale weather station, are from 12 to 36 m; the temperatures were in the ranges from 3.2 to

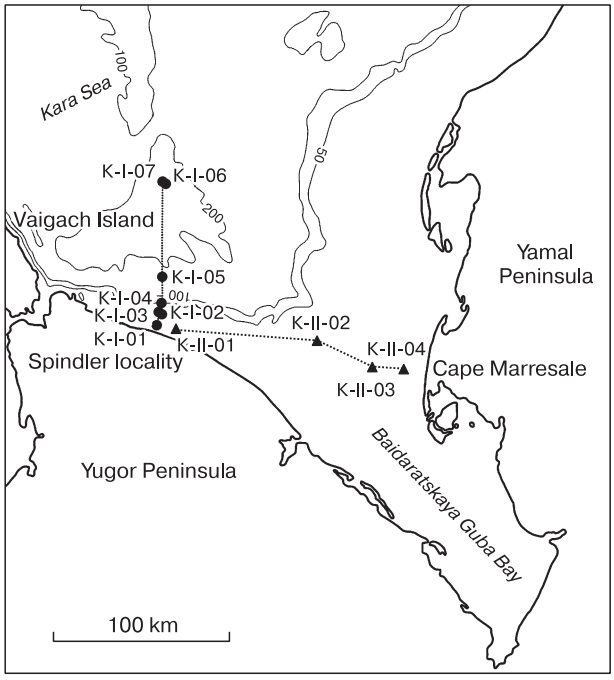

Fig. 1. Location map of sampling profiles K-I (northward from Spindler locality) and K-II (eastward from Spindler to Marresale Cape).

5.9 °C in the near-surface water and from –1.05 to 3.15 °C in the bottom water, and from –0.9 to 2.0 °C in the bottom sediments [*Vanstein et al., 2008*].

Particle sizes were measured using a Malvern *Mastersizer 3000* laser diffraction particle size analyzer by the liquid dispersion method [*Kurchatova and Rogov, 2014*]. The mineralogy of the samples was studied on a Bruker *D2 PHASER* X-ray powder diffractometer, and the diffraction patterns were processed using the *Eva* and *Topaz* software packages. Cryogenic weathering of the sediments was inferred from mineralogy of the selected sample fractions using the coefficient of cryogenic contrast (*CCC*) [*Konishchev and Rogov, 1994*]:

$$CCC = \frac{Q_1/F_1}{Q_2/F_2},$$

where Q_1 and F_1 are the percentages of quartz and feldspar grains in the 0.05–0.01 mm fraction; Q_2 and F_2 are the respective percentages in the 0.10–0.05 mm fraction.

The sediment microstructure and compositions were studied on a Hitachi *TM3000* tabletop electron microscope equipped with an Oxford Swift *ED3000* EDS system. The analyses were performed with a special focus on microstructures and on quartz grain morphology as diagnostic of cryogenic weathering in Quaternary sediments [*Rogov, 2009*].

RESULTS

Particle sizes

The analyzed samples of the Kara shelf sediments have high percentages (50 to 74 %) of the silt

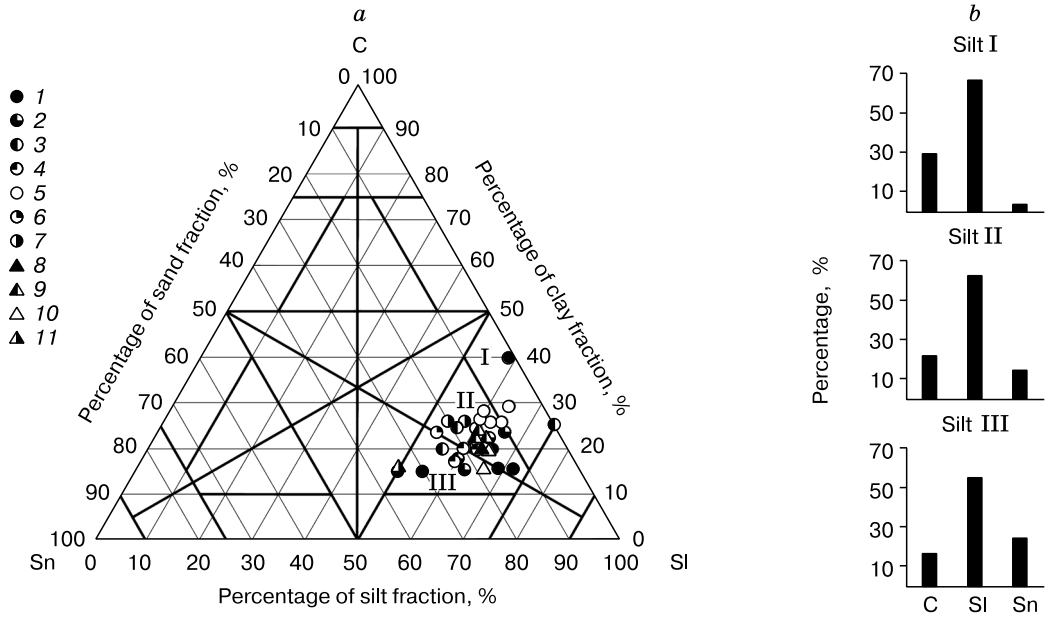

Fig. 2. Diagram of particle size distribution in analyzed samples from the Kara Sea shelf [*Frolov, 1993*] (*a*) and particle-size histograms of different silt families (*b*).

C = clay fraction (<0.005 mm); Sl = silt fraction (0.005–0.05 mm); Sn = sand fraction (0.05–2.5 mm).
I = clay-rich silt; II = sandy clay-rich silt; III = sandy-clayey silt. Symbols correspond to numbers of profiles and core samples: *1* = K-I-01; *2* = K-I-02; *3* = K-I-03; *4* = K-I-04; *5* = K-I-05; *6* = K-I-06; *7* = K-I-07; *8* = K-II-01; *9* = K-II-02; *10* = K-II-03; *11* = K-II-04.

fraction, 0.005–0.05 mm, and can be classified as silt varieties of more or less fine grain sizes (Fig. 2) [*Frolov, 1993*]. They are *clay-rich silt* with >25 % of clay particles and <10 % of sand particles; *sandy clay-rich silt* with <25 % of clay particles and <20 % of sand particles; and *sandy-clayey silt* with the respective percentages of <20 % (clay) and >25 % (sand). The sorting coefficient is within 0.5 in all samples, i.e., the sediments are well sorted.

The three lithological silt varieties correlate with sea and core depths (Fig. 3): sandy-clayey silt occurs in shallow water, within core depths of 30 cm, sandy clay-rich silt is found throughout the section, including the shallow-water section parts, while clay-rich silt mostly occurs in deepwater shelf and occupies the whole section of cores sampled at >140 m water depths. Dark gray dense clay-rich silt was found also near the shore of the Yugor Peninsula and may be of the same origin as Pleistocene clay in the coastal outcrops at the Spindler locality.

The lithogenetic features of the sediments were interpreted using Gostintsev's (Fig. 4) and Passega's (Fig. 5) diagrams. The skewness (Sk) and kurtosis (Kt) coefficients in the Gostintsev diagram record mechanic sorting of clastic particles in different facies on the basis of grain sizes [*Gostintsev, 1989*]. According to the results, two thirds (20 out of 33) of the samples can be classified as deposited under high-energy wave action and tides (Fig. 4, *a*, *b*); 7 samples are sediments of slow currents and stagnant zones (*e*); 5 samples were deposited in shallow-marine conditions (*d*), and one sample falls within the filed of fluvial and floodplain facies (*c*).

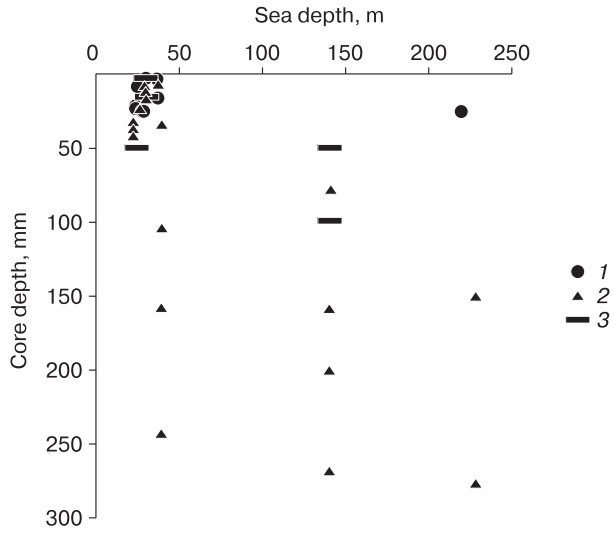

Fig. 3. Distribution of lithologies as a function of sea depth and core depth.

1 – sand-clayey silt; *2* – sandy clay-rich silt; *3* – clay-rich silt.

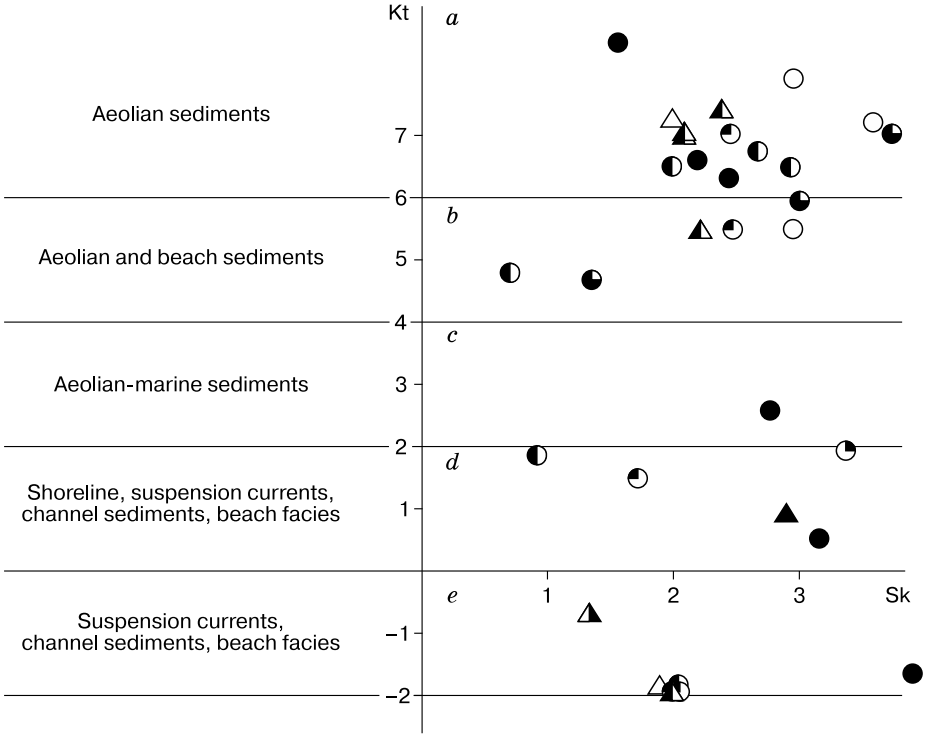

Fig. 4. Gostintsev's diagram of deposition environments.

a – marine sediments, high-energy wave action and tides; *b* – marine sediments, high-energy wave action; *c* – fluvial and floodplain sediments; *d* – broad mouth parts of rivers, shallow water, river pools, marine facies; *e* – slow currents, stagnant zones, lakes and weathering profiles. Sk = skewness; Kt = kurtosis. Symbols are same as in Fig. 2.

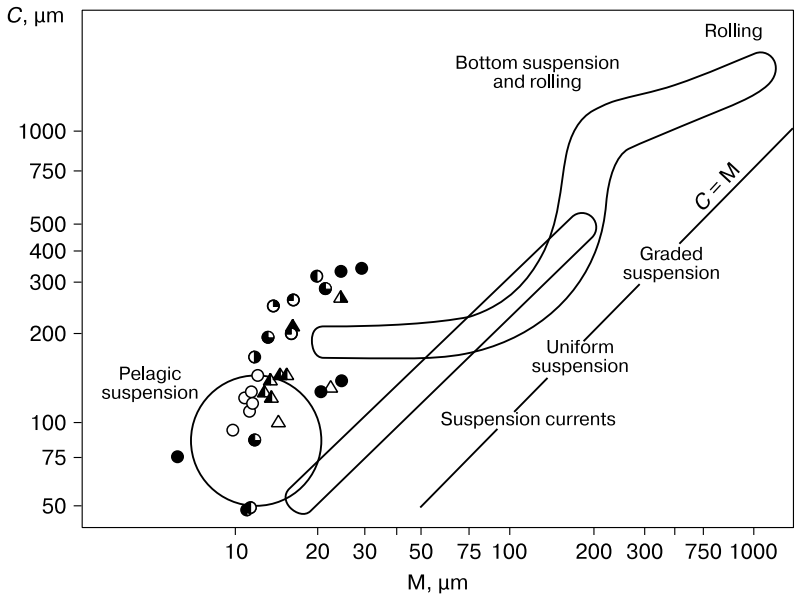

Fig. 5. Passega's *C*–M diagram: hydraulic conditions of sediment formation based on grain sizes.

C = 99 % percentile; M = the median of the particle-size distribution. Symbols are same as in Fig. 2.

In Passega's *C*–M diagram the median (M) of the grain-size distribution is plotted against 99%-th percentile (*C*) which characterizes the maximum lift force of a stream [*Passega and Byramjee, 1969*], assuming that the sediments carried by a stream either roll on the bottom or are entrained with suspension. The diagram shows that all sediments belong to the fields of pelagic and graded suspension and were deposited in still water.

Mineralogical analysis

The sediments represent three types of deposition environments: they are of marine, coastal, and continental facies with clay contents of 30–40 wt.%, 20–30 wt.%, and 10–20 wt.%, respectively, which correspond to clay-rich, sandy clay-rich, and sandy-clayey silt lithologies (Fig. 6). The deposition environments are inferred from relative proportions of light-fraction minerals in a feldspar-plagioclase-qu-

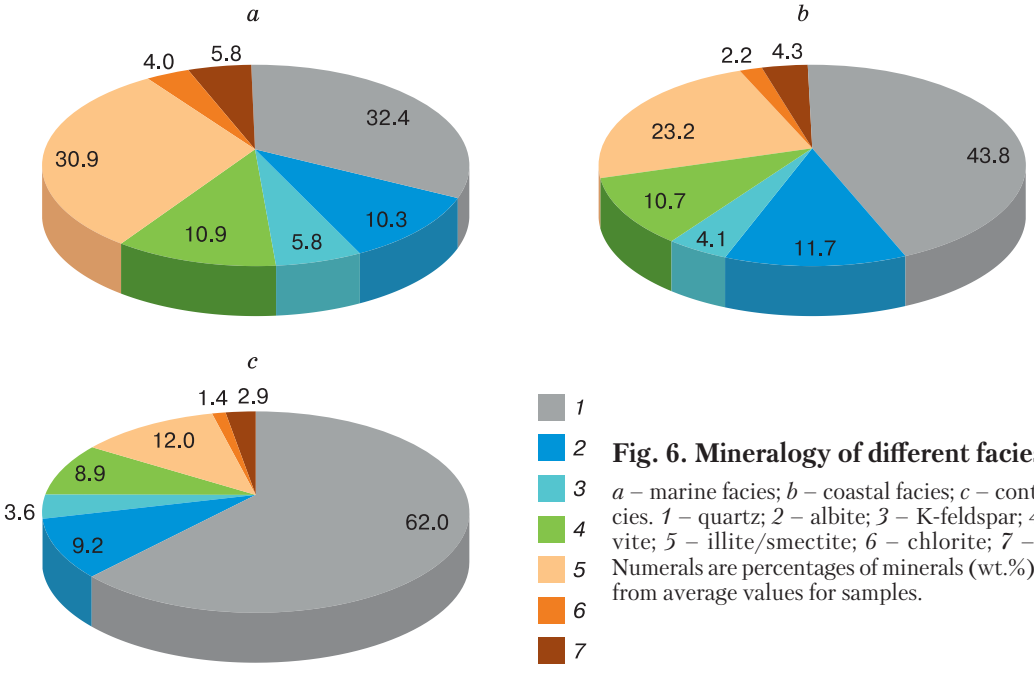

Fig. 6. Mineralogy of different facies.

a – marine facies; *b* – coastal facies; *c* – continental facies. *1* – quartz; *2* – albite; *3* – K-feldspar; *4* – muscovite; *5* – illite/smectite; *6* – chlorite; *7* – kaolinite. Numerals are percentages of minerals (wt.%) calculated from average values for samples.

artz assemblage. High percentages of quartz relative to clay ($Q/\Sigma_{clay} > 1$), and feldspar ($Q/F_s > 2.5$) are indicative of clastic origin. Average values of these ratios in the analyzed bottom sediment samples are, respectively, $Q/\Sigma_{clay} = 4.0$ (3.3–4.6) and $Q/F_s = 4.9$ (4.4–5.5) for continental facies, $Q/\Sigma_{clay} = 1.5$ (1.2–1.8) and $Q/F_s = 2.9$ (2.5–3.2) for coastal deposits, and $Q/\Sigma_{clay} = 0.8$ (0.1–1.0) and $Q/F_s = 2.0$ (2.0–2.1) for sediments deposited in submarine conditions. The clay minerals in all lithological types are mainly

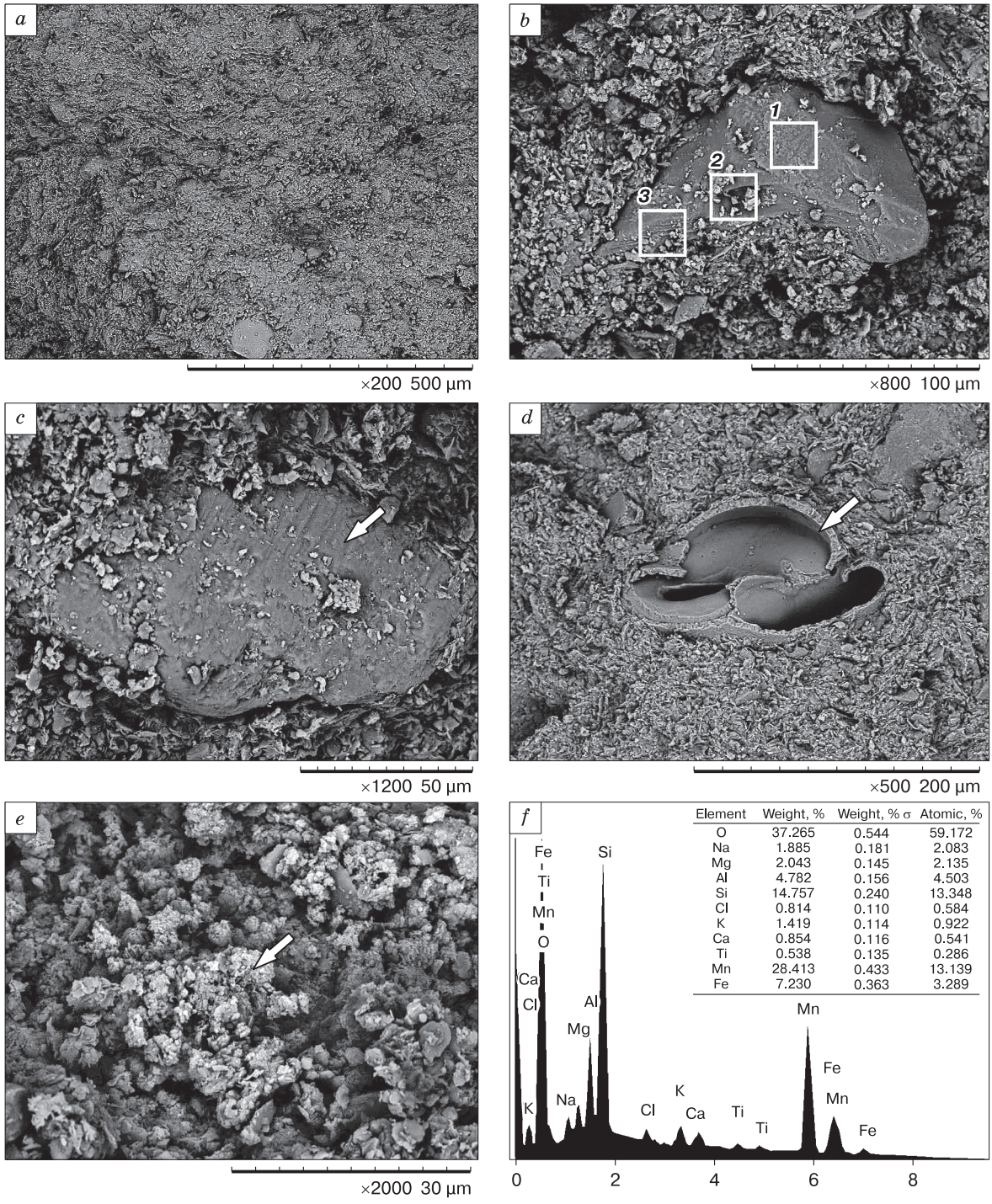

Element	Weight, %	Weight, % σ	Atomic, %
O	37.265	0.544	59.172
Na	1.885	0.181	2.083
Mg	2.043	0.145	2.135
Al	4.782	0.156	4.503
Si	14.757	0.240	13.348
Cl	0.814	0.110	0.584
K	1.419	0.114	0.922
Ca	0.854	0.116	0.541
Ti	0.538	0.135	0.286
Mn	28.413	0.433	13.139
Fe	7.230	0.363	3.289

Fig. 7. Microstructure of clay-rich silt:

a – wavy texture; *b* – quartz particle (*1* – cleavage, *2* – conchoidal fracture, *3* – parallel striation); *c* – microcline with a stepped surface concordant with cleavage; *d* – gastropod shell; *e* – iron-manganese concretions; *f* – contents of elements and EDS element patterns for an iron-manganese concretion.

mixed-layer illite-smectite typical of the Arctic shelf deposits [*Levitan et al., 2004*].

Microscopy

The clay-rich silt sediments have high clay contents and are dense and homogeneous (Fig. 7). Their microstructures reveal wavy bedding, mainly due to orientations of mica particles. The clay-rich samples retrieved at the greatest sea depths (220–228 m) enclose iron-manganese concretions produced by postdepositional alteration, which are common to hemipelagic sediments of the Arctic seas [*Bogdanov*

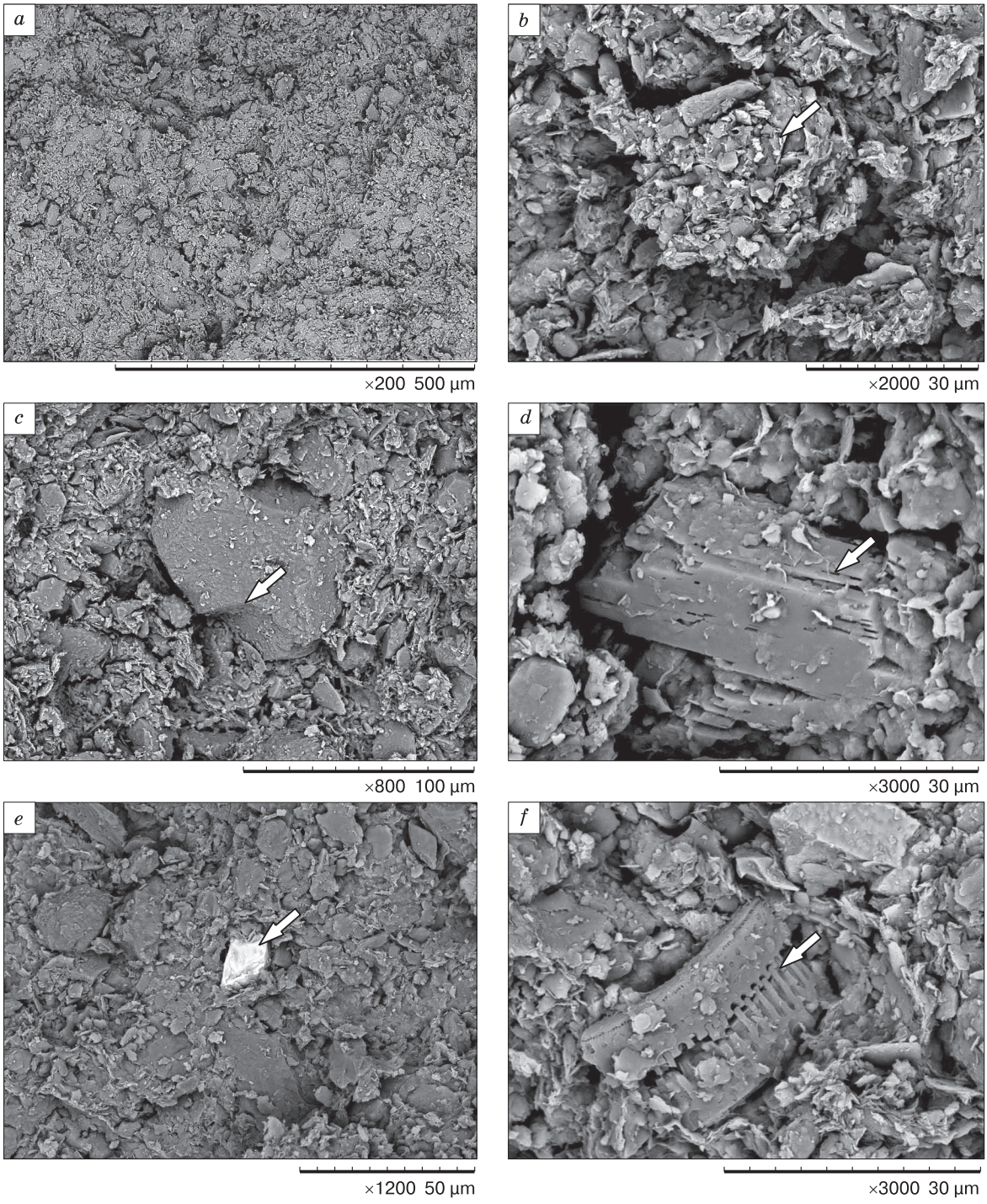

Fig. 8. Microstructure of sandy clay-rich silt:

a – mosaic texture; *b* – clay aggregate; *c* – quartz particle with conchoidal fracture; *d* – feldspar particle with cleavage; *e* – a secondary REE phase; *f* – diatom frustules.

et al., 1994]. Microscopy under relatively large magnification reveals individual >100 μm angular quartz particles with conchoidal fracture, possibly, resulting from frost weathering [*Rogov, 2009; Udayaganesan et al., 2011; Müller and Knies, 2013; Woronko, 2016*].

Sandy clay-rich silt has a heterogeneous mosaic texture with separate particles set into a clay matrix filling the intergranular space (Fig. 8). The clay material, devoid of distinct orientations, forms coats on mineral grains and accumulates along grain boundaries making up a skeletal microstructure. Sediments of this type contain abundant aggregates from 30 to 75 μm. Both fine (<75 μm) and coarse (>100 μm) quartz particles are angular, with conchoidal fracture. Some feldspar grains bear signatures of dissolution and enclose colloidal LREE (La, Ce, Nd) phases typical of marine deposits.

Sand-clay silt samples are porous, with clay making isolated flakes in interstices (Fig. 9). Most of coarser particles (>100 μm) are more rounded than the finer ones and bear traces of cleavage and conchoidal fracture. The samples of sandy silt contain spherical hydrotroilite inclusions, most often next to clay flakes.

The sediment microstructures are free from effects of relict or present permafrost, despite negative temperatures of bottom water in the shallow shelf (within 20–30 m sea depths). The *CCC* ratios are the highest (0.9) in the core samples from the Biadaratskaya Bay, which mainly consist of fine silt particles (50–75 μm) and contain frost-affected quartz grains of different particles sizes from fine sand to fine silt. Therefore, the sediments likely were exposed to freezing in subaerial conditions of continental margins but were redeposited after erosion of Pleistocene terraces by high-energy tides. Coarser quartz particles of the sand fraction are quite well rounded like those of fluvial deposits.

Clay-rich and sandy clay-rich samples from deeper shelf abound in >100 μm angular quartz particles with conchoidal fracture, enclose iron-manganese concretions, and contain abundant gastropod shells and diatom frustules. This is evidence of their marine genesis and inputs of ice-rafted debris material [*Lisitsyn, 2010*].

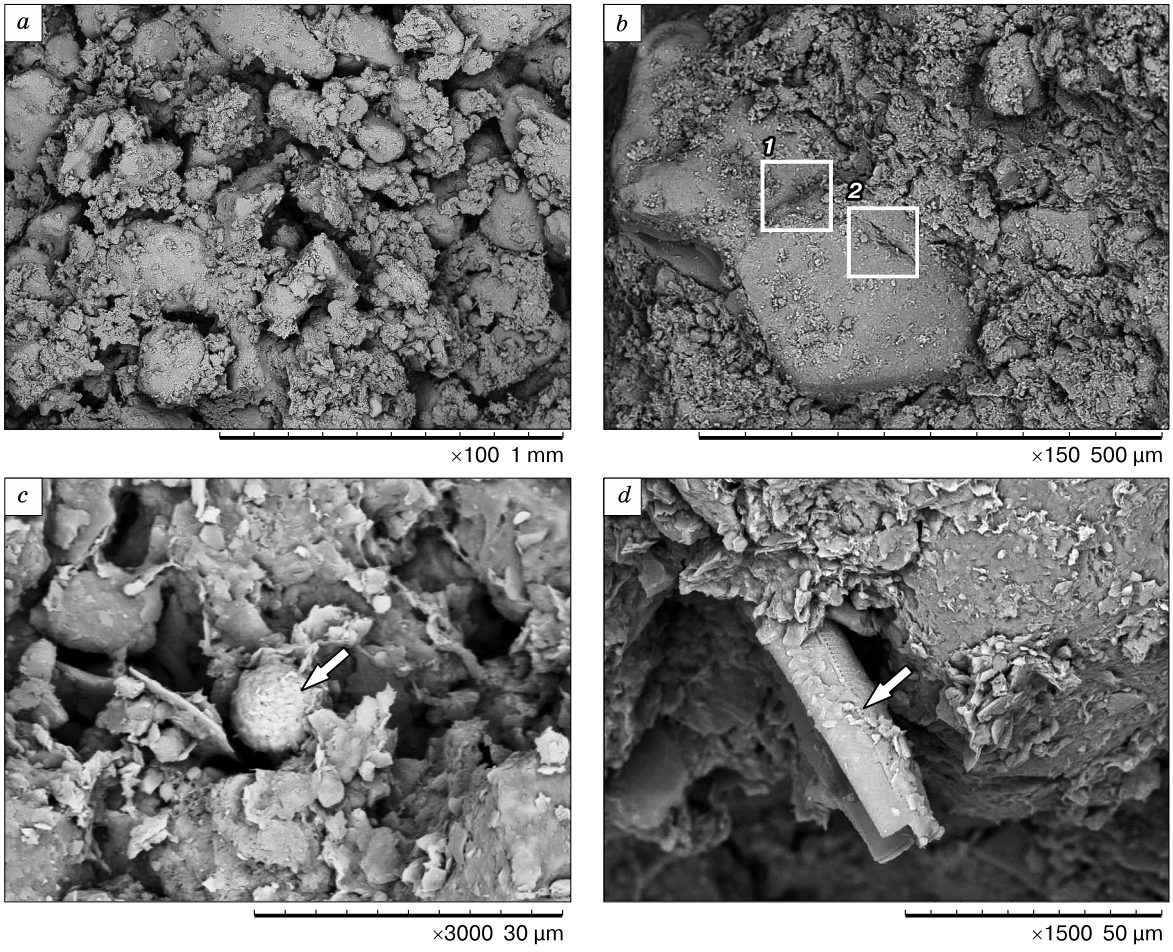

Fig. 9. Microstructure of sandy-clayey silt:

a – porous sediment; *b* – quartz particle (*1* – conchoidal fracture, *2* – cleavage); *c* – colloidal hydrotroilite; *d* – diatom frustule.

CONCLUSIONS

1. The analyzed bottom sediments from the eastern Kara shelf are clay-rich, sandy clay-rich, and sandy-clayey varieties of silt according to particle-size distribution. In the diagrams of Gostintsev and Passega, sediments show origin in high- or low-energy environments but plot generally in the field of still water. The shelf sediments sampled at shallow sea depths are of coastal (<50 m) or marine (>50 m) facies; the coastal facies are locally redeposited continental sediments.

2. The mineralogy of shelf sediments correlates with their marine, coastal, or continental origin. The three facies correspond to the three types distinguished on the basis of particle size distribution: clay-rich and sandy clay-rich silt varieties are of marine and coastal facies, respectively, while sandy-clayey silt was originally deposited in continental conditions.

3. The microstructures of the analyzed core samples look free from signatures of freezing in relict or present permafrost. The frost imprints revealed from quartz grain morphology in shallow-water bottom sediments from the eastern Kara shelf are inherited. Sandy-clayey silt includes <75 μm angular quartz grains with conchoidal fracture typical of redeposited subaerial facies of Late Pleistocene terraces. The clay-rich and sandy clay-rich varieties contain >100 μm particles with cleavage and conchoidal fracture which could be transported together with ice-rafted debris.

The study was supported by the Russian Foundation for Basic Research (Project 18-05-00376).

References

Bogdanov, Yu.A., Gorshkov, A.I., Gurvich, E.G., Bogdanova, O.Yu., Dubinina, G.I., Ivanov, G.V., Isaeva, A.B., Muraviev, K.G., 1994. Iron-manganese concretions of the Kara Sea. Okeanologiya (Oceanography) 34 (5), 789–800.

Danilov, I.D., 1992. The Arctic cryogenic marine sediments and their main deposition stages, in: Mesozoic and Cenozoic Geological history of the Arctic. VNIIOkeangeologiya, St. Petersburg, Book II, pp. 29–37. (in Russian)

Frolov, V.T., 1993. Lithology. Book 2. Moscow University Press, Moscow, 432 pp. (in Russian)

Gostintsev, K.K., 1989. Guidelines for Fractional Particle Size Analysis by the Sedimentation Method. VNIGRI, Leningrad, 181 pp. (in Russian)

Gritsenko, I.I., Bondarev, V.N., 1994. Subsea Permafrost, Gas Hydrates and Gas Pockets in Cenozoic Sediments of the Barents, Pechora and Kara Seas: Preprint 14th World Petroleum Congress, Stavanger, topic 6. – URL: https://www.onepetro.org/conference-paper/WPC-26159.

Kassens, H., Bauch, H., Drachev, S., Gierlichs, A., Niessen, F., Taldenkova, E., Roudoy, A., Thiede, J., Wessels, M., 2000. The Transdrift VIII Expedition to the Laptev Sea: the shelf drilling campaign of "Laptev Sea System 2000", in: Sixth Workshop on Russian/German Cooperation: Laptev Sea System. Terra Nostra 8, 39–40.

Konishchev, V.N., Rogov, V.V., 1994. Methods of Permafrost Research. Moscow University Press, Moscow, 135 pp. (in Russian)

Kurchatova, A.N., Rogov, V.V., 2014. New methods and approaches to the study of the granulometric and morphological composition of cryogenic soils. Inzhinernye Izyskaniya (Engineering Survey), No. 5–6, 58–63.

Levitan, M.A., Burtman, M.V., Demina, L.L., Krupskaya, V.V., Sedykh, E.M., Chudetsky, M.Yu., 2004. Holocene Deposition History in the southern Kara Sea. Litologiya i Poleznye Iskopaemye (Lithology and Mineral Deposits), No. 6, 651–666.

Lisitsyn, A.P., 2010. Marine ice-rafting as a new type of sedimentogenesis in the Arctic and novel approaches to studying sedimentary processes. Russian Geology and Geophysics 51 (1), 12–47.

Maslov, A.D., 1988. Cryodiagenesis in marine deposition, in: Problems of Geocryology. Nauka, Moscow, pp. 41–55. (in Russian)

Melnikov, V.P., Fedorov, K.M., Wolf, A.A., Spesivtsev, V.I., 1998. Analysis of the possible scenario of the formation of bottom ice mounds on the shelf of the Pechora Sea. Kriosfera Zemli (Earth's Cryosphere) II (4), 51–57.

Melnikov, V.P., Spesivtsev, V.I., 1995. Geotechnical and Geocryological Conditions of the Barents and Kara Shelves. Nauka, Novosibirsk, 195 pp. (in Russian)

Müller, A., Knies, J., 2013. Trace elements and cathodoluminescence of detrital quartz. Climate of the Past 9, 2615–2630.

Neizvestnov, Ya.V., Kozlov, S.A., Kondratenko, A.V., 2012. Variability and heterogeneity of mechanical properties of recent sediments in the Arctic shelf. Zapiski Gornogo Instituta (Reports of the Mining Institute) 197, 203–208.

Neizvestnov, Ya.V., Reshetova, O.V., 1990. Engineering geology of the Arctic shelves, in: Engineering Geology of the USSR. Shelves of the USSR. Nedra, Moscow, pp. 44–90. (in Russian)

Passega, R., Byramjee, R., 1969. Grain-size image of clastic deposits. Sedimentology 13 (3–4), 233–252.

Rogov, V.V., 2009. Fundamentals of Cryogenesis. Geo Publishers, Novosibirsk, 203 pp. (in Russian)

Rokos, S.I., 2008. Geotechnical features of near-surface overpressure zones in shelf reservoirs of the Pechora and southern Kara Seas. Inzhenernaya Geologia (Engineering Geology), No. 4, 22–28.

Shpolyanskaya, N.A., Streletskaya, I.D., Surkov, A.V., 2006. Cryolithogenesis in Arctic shelf (recent and relict). Kriosfera Zemli (Earth's Cryosphere) X (3), 49–60.

Soloviev, V.A., 1988. Barents Sea Shelf, in: Geocryology of the USSR. European USSR. Nedra, Moscow, pp. 259–262. (in Russian)

Udayaganesan, P., Angusamy, N., Gujar, A.R., Rajamanickam, G.V., 2011. Surface microtextures of quartz grains from the central coast of Tamil Nadu. J. Geol. Soc. India 77, 26–34.

Vanstein, B.G., Zakharov, V.Yu., Kaminsky, D.V., Kasyankova, N.A., Kuznetsova, M.V., Serov, P.I., Koss, A.V., 2008. Marine surveys of 2007 in the southwestern Kara Sea. Surveys of 2007 by VNIIOkeangeologiya, in: Annual Review, VNIIOkeangeologiya, St. Petersburg, pp. 44–51. (in Russian)

Woronko, B., 2016. Frost weathering versus glacial grinding in the micromorphology of quartz sand grains: Processes and geological implications. Sedimentary Geology 335, 103–119.

Received January 18, 2018
Revised version received January 22, 2019
Accepted March 10, 2019